Title
Distinct functions for IFT140 and IFT20 in opsin transport

Journal
Cytoskeleton, 71(5)

ISSN
1949-3584

Authors
Crouse, Jacquelin A
Lopes, Vanda S
SanAgustin, Jovenal T
et al.

Publication Date
2014-05-01

DOI
10.1002/cm.21173

Peer reviewed

Published in final edited form as:
Cytoskeleton (Hoboken). 2014 May ; 71(5): 302–310. doi:10.1002/cm.21173.

Distinct functions for IFT140 and IFT20 in opsin transport.

Jacquelin A. Crouse[1], **Vanda S. Lopes**[2], **Jovenal T. SanAgustin**[1], **Brian T. Keady**[1], **David S. Williams**[2], and **Gregory J. Pazour**[1,‡]

[1]Program in Molecular Medicine, University of Massachusetts Medical School, Biotech II, Suite 213, 373 Plantation Street, Worcester, MA 01605

[2]Jules Stein Eye Institute, UCLA David Geffen School of Medicine, 200 Stein Plaza, Los Angeles, CA 90095-7008

Abstract

In the vertebrate retina, light is detected by the outer segments of photoreceptor rods and cones, which are highly modified cilia. Like other cilia, outer segments have no protein synthetic capacity and depend on proteins made in the cell body for their formation and maintenance. The mechanism of transport into the outer segment is not fully understood but intraflagellar transport (IFT) is thought to be a major mechanism for moving protein from the cell body into the cilium. In the case of photoreceptor cells, the high density of receptors and the disk turnover that occurs daily necessitates much higher rates of transport than would be required in other cilia. In this work, we show that the IFT complex A protein IFT140 is required for development and maintenance of outer segments. In earlier work we found that acute deletion of *Ift20* caused opsin to accumulate at the Golgi complex. In this work we find that acute deletion of *Ift140* does not cause opsin to accumulate at the Golgi complex but rather it accumulates in the plasma membrane of the inner segments. This work is strong support of a model of opsin transport where IFT20 is involved in the movement from the Golgi complex to the base of the cilium. Then, once at the base, the opsin is carried through the connecting cilium by an IFT complex that includes IFT140.

Keywords

cilia; flagella; intraflagellar transport; photoreceptor; vision

Introduction

The outer segments of vertebrate rods and cones are highly modified cilia and are responsible for absorbing light as the first step in the visual signal transduction cascade. These cilia, like all cilia and flagella, lack the capacity for protein synthesis and rely on proteins synthesized in the cell body and transported into the organelle for their development and maintenance. During development, photoreceptor cells assemble a primary cilium that is structurally similar to other primary cilia in vertebrates. This cilium then differentiates to become the outer segment by the movement of large amounts of lipid and membrane proteins into the cilium. In mouse, this process starts about 6.5 days after birth and continues

‡Corresponding Author, Telephone: 508 856 8078, gregory.pazour@umassmed.edu.

until approximately post natal day (P) 20 when the outer segments achieve adult proportions [LaVail, 1973; Fei, 2003]. The high level of membrane and membrane protein transport continues in the adult as approximately 10% of the outer segment is shed from the distal tip each day and must be replaced by new disks that form at the base of the outer segment. In mouse, it is estimated that approximately 4300 molecules of opsin must be transported through the connecting cilium each minute to replace the opsin lost through disk shedding [Williams, 2002]. In fish and frogs, the outer segment diameters are much larger and the transport requirements approach 50,000 per minute [Young, 1967; Besharse and Horst, 1990]. The molecular mechanism driving the transport of opsin photopigments from the Golgi complex to the cilium is largely unknown but evidence points to the intraflagellar transport (IFT) systems as an important player [Insinna and Besharse, 2008; Bhowmick et al., 2009].

The intraflagellar transport system is required for the assembly of most types of eukaryotic cilia including the outer segments of photoreceptor rods and cones [Marszalek et al., 2000; Pazour et al., 2002]. During IFT, large protein complexes called IFT particles or trains are transported from the cell body to the ciliary tip by kinesin-2 [Cole et al., 1998] and from the tip back to the cell body by cytoplasmic dynein-2 [Pazour et al., 1999]. The particles themselves are composed of more than 20 subunits organized into two subcomplexes called A and B. The B complex appears to be critically important for cilia assembly as null mutations in most components block ciliary assembly [Pazour et al., 2000; Brazelton et al., 2001] while the A complex appears to be less important for cilia assembly but play roles in retrograde transport [Iomini et al., 2009]. However, complex A also is important for anterograde transport as it links heterotrimeric kinesin to the IFT particle for transport from the cell body to the ciliary tip [Ou et al., 2007] and the knockdown of IFT-A components prevents the delivery of Tulp3 and the G-protein coupled receptors SSTR3 and MCHR1 to the cilium [Mukhopadhyay et al., 2010]. The IFT particles are also associated with a third complex called the BBSome that is required for delivery of a subset of seven-transmembrane receptors into the cilia [Berbari et al., 2008] and the selective removal of membrane-associated proteins that are not normally found in cilia [Lechtreck et al., 2009]. The IFT particles are highly conserved throughout the eukaryotic kingdom and are thought to serve as motor adaptors to connect cargos that need to be transported into and along cilia to the molecular motors.

Why the IFT particle requires more than 20 unique subunits is completely unknown at this time. The high degree of conservation of the IFT particle proteins suggests that each of the IFT subunits has unique critical functions to play in the assembly of cilia and their maintenance. To understand the unique functions of the IFT particle proteins, we are creating mutant mice carrying floxed alleles of the *Ift* genes and examining how the loss of these genes affects the assembly and stability of the photoreceptor outer segments. In the present work, we have focused on the complex A protein IFT140. The role of complex A proteins in photoreceptor outer segment development and maintenance has not been extensively examined. Prior work in zebrafish suggested that *Ift140* was not a critical player in ciliary assembly or outer segment development [Tsujikawa and Malicki, 2004] but maternal contributions of protein could mask the true phenotype in fish development. In

humans, the loss of IFT140 leads to Mainzer-Saldino syndrome and Jeune asphyxiating thoracic dystrophy, rare syndromes where patients are affected by chronic renal failure, early-onset severe retinal dystrophy and skeletal dysplasias [Perrault et al., 2012; Schmidts et al., 2013]. In mouse, deletion of *Ift140* from kidney collecting ducts strongly affected, but did not completely block primary cilia assembly and resulted in cystic kidney disease [Jonassen et al., 2012].

Here, we compare the deletion of *Ift140* to our prior work on the deletion of *Ift20*. IFT20 is an IFT complex B protein that is also associated with the Golgi complex. Based on the Golgi localization and phenotypes that resulted from the partial knockdown of IFT20 in cultured cells we proposed that IFT20 was important for transport between the Golgi and the cilium [Follit et al., 2006]. The deletion of *Ift20* in cone cells lead to their degeneration such that cone numbers were reduced at P28 and the cells were mostly gone by P70. Acute deletion of *Ift20* in rods lead to an accumulation of rhodopsin at the Golgi complex before photoreceptor cell degeneration supporting a role for IFT20 in the transport of opsin between the Golgi and the connecting cilium [Keady et al., 2011]. However, concerns that this may be an indirect effect caused by the failure of opsin to be trafficked through the connecting cilium caused us to repeat this experiment using IFT140, an IFT protein that is not Golgi localized. In the current study we show that loss of IFT140 from cone cells leads to a degenerative phenotype similar to what was observed with loss of IFT20, except with slower progression. Interestingly, the acute loss of IFT140 caused opsin to accumulate in the plasma membrane of the inner segment in contrast to the Golgi accumulation that occurred when IFT20 was acutely lost. These data strongly support differential roles of IFT20 and IFT140 in the transport of rhodopsin through the photoreceptor cell.

Results

Photoreceptor rod and cones are composed a light detecting outer segment, which is connected to the inner segment of the cell body by the connecting cilium. The inner segment is the biosynthetic compartment of the cell and contains the mitochondria in its distal region and the Golgi apparati in its proximal region. The inner outer segments lie distal to the cell body; the photoreceptor cell nuclei are packed together to form the outer nuclear layer of the retina. A short axon bears a synapse, which harbors dendrites of second-order neurons within an invagination (Fig 1A). The primary organization of the photoreceptor layer of the retina is driven by the rod cells, which are the most abundant photoreceptor cell in the mouse retina. The cones are organized with their nuclei in the most distal row of the outer nuclear layer, and their outer segments typically start in the middle of the rod inner segment layer. IFT proteins typically are found dispersed throughout the inner segment with concentrations in the peri-basal body region at the base of the outer segment and in a second smaller pool at the distal end of the connecting cilium [Pazour et al., 2002]. It was reported that IFT140 was different with the largest pool at the distal end of the connecting cilium and only a minor amount in the peribasal body region [Sedmak and Wolfrum, 2010]. In contrast to Sedmak and Wolfrum, we find that the major pool of IFT140 is at the base of the cilium with only a small amount in the cilium itself (Fig 1B,B’). It is likely that the distribution of IFT140 would be similar in cones as it is in rods but this is not certain. To analyze the distribution of IFT140 in cones, dispersed retinal cells and retina sections were stained for

IFT140, cilia and cone opsin. Cone opsin-positive cells showed the strongest signal at the base of the cilium with additional label in the connecting cilium and some on the microtubules of the outer segment (Fig 1C,D). Thus, in both rods and cones, the distribution of IFT140 is similar to the distribution of other IFT proteins and could be involved in transport through the connecting cilium.

Germline deletions of *Ift140* cause embryonic lethality at mid gestation before the development of the outer segments of photoreceptor rods and cones. To understand the role of IFT140 in the formation of the outer segment, we used embryonic stem cells generated by the Knockout Mouse Project to create a floxed allele. This allele has exon 7 flanked by loxP sites. Cre deletion of exon 7 is predicted to create a null allele as the splicing of exon 6 to exon 8 would cause a frameshift and subsequent translation termination. This appears to be the case as no protein is detected from the deleted allele using an antibody directed against the C-terminal end of the protein [Jonassen et al., 2012]. To delete this allele in photoreceptor cells, we used Cre driven by the human red-green opsin promoter (HRGP-Cre). This Cre is expressed in M-opsin positive cone photoreceptors. There does not appear to be any expression of HRGP-Cre in rod cells (Fig 2A) and no deleterious effects on them [Keady et al., 2011]. Many Cre lines have pathology in the cells where Cre is expressed even without a floxed allele being present [Lee et al., 2006; Jimeno et al., 2006]. This does not appear to be the case with HRGP-Cre as we do not detect any cone opsin at the ribbon synapse in Cre-positive control animals nor do we see a reduction of cone cell numbers in older animals. However, to ensure that the phenotypes we observe are not caused by non-specific effects of Cre expression, the control animals in this study were *HRGP-Cre*+, $Ift140^{flox/+}$.

HRGP-Cre expression initiates around postnatal (P) day 6 as the outer segments of photoreceptors begin to develop [Le et al., 2004]. To understand how the loss of *Ift140* affects the development and maintenance of the outer segments, retinas were harvested at P11, P28 and P70. Cre recombinase was robustly detected in the nuclei of both control (*HRGP-Cre*+, $Ift140^{flox/+}$) and experimental (*HRGP-Cre*+, $Ift140^{flox/null1}$) animals at all time points. At P11 the outer segments were still forming and looked similar in the control and experimental animals (Fig 2A). Opsin was detected in the inner segments and nuclear layer in both the control and experimental animals. At P28 outer segment development is normally completed. The opsin seen in the inner segments and nuclear layers at P11 was mostly cleared from control animals but remained in theses layers as well as the outer plexiform layer of retinas from the experimental animals. The outer segments of the experimental animals are malformed and it is hard to distinguish the inner and outer segments. At P70, significant degeneration was occurring in the experimental animals as there was a large amount of opsin in the inner segments, surrounding the nuclei and at the synapse. While there was a trend towards cone cell loss, the number of cones in the experimental animals was not significantly reduced as compared to the controls at any time point.

The pathology seen in the experimental animals indicates that IFT140 is required in cone cells but because HRGP-Cre expression initiates as the outer segments are developing, the effects on development verses maintenance are hard to separate. To understand the role that

IFT140 plays in maintenance and the delivery of opsin to the outer segment, we used the tamoxifen-inducible CAG-CreER to induce the deletion of *Ift140* in fully differentiated cells. This Cre is widely expressed but is not active until it binds tamoxifen and becomes nuclear localized. In cell culture we determined that 48 hr after tamoxifen administration *Ift20* levels were reduced to about one half. Very similar effects were observed in the retina of mice treated with tamoxifen [Keady et al., 2011]. Similarly we found that *CAG-CreER+*, $Ift140^{flox/null1}$ animals treated with tamoxifen had about a 50% reduction in IFT140 protein in the retina 48 hr after the drug was administered (41±20 percent remaining, n=8). This acute loss of IFT140 caused significant amounts of opsin to accumulate in the inner segments and the nuclear layer that was not observed in control animals (Fig 3A). The distribution of opsin in the tamoxifen treated *CAG-CreER+*, $Ift140^{flox/null1}$ animals was quite different from what we had observed prior when *CAG-CreER+*, $Ift20^{flox/null1}$ animals were examined. When *Ift20* was deleted, the opsin was mostly found in the inner segment just above the nuclear layer where it colocalized with Golgi markers (see Fig 4 in [Keady et al., 2011]). To quantitate the difference between the opsin localization in *Ift20* deleted photoreceptor cells and *Ift140* deleted cells, additional retinas were collected and analyzed by immunogold electron microscopy (Fig3B and C). With both *Ift20* and *Ift140*, the loss of the IFT caused a significant increase in the gold particle density in the inner segment of the cells (Fig 3C). However, the location of the gold particles was different in the two genotypes. When *Ift20* was deleted, the gold particles were clustered just above the outer limiting membrane over the Golgi stacks. When *Ift140* was deleted, the gold was concentrated along the plasma membranes of the inner segments.

Discussion

In this work we demonstrate that the IFT complex A gene *Ift140* is required for the development and maintenance of the outer segment of photoreceptor cells. The degeneration in *Ift140* cells was similar to what we previously observed when the IFT complex B gene *Ift20* was deleted using the same Cre driver but the degeneration was less extreme in the *Ift140* case. This difference is consistent with what we observed in the kidney where deletion of *Ift20* and *Ift40* both caused post natal cystic kidney disease with very similar kinetics. However, ciliary assembly was totally blocked by the *Ift20* deletion whereas the *Ift140* deletion did not completely block ciliary assembly and short cilia remained [Jonassen et al., 2008; Jonassen et al., 2012]. The slower degeneration in *Ift140*-deleted cone cells is also consistent with observations of the function of complex A verses complex B in other organisms. In *Caenorhabditis*, complex B mutations tend to block ciliary assembly whereas complex A mutations result in normal length cilia that are filled with a poorly defined material [Perkins et al., 1986]. In *Chlamydomonas*, IFT B mutations block ciliary assembly [Pazour et al., 2000; Brazelton et al., 2001] whereas IFT A mutations result in defects in retrograde transport [Iomini et al., 2009]. Our results are more consistent with a failure to transport material through the connecting cilium rather than a defect in retrograde transport, consistent with evidence that complex A also plays roles in anterograde transport. Significantly, complex A is the site where heterotrimeric kinesin II binds to the IFT particle [Ou et al., 2007]. Photoreceptor cells also express another kinesin II, homodimeric Kif17and this likely binds complex B [Ou et al., 2007]. Both kinesins are important in photoreceptor

cells [Insinna et al., 2009] but heterotrimeric kinesin appears to be the major carrier for rhodopsin [Marszalek et al., 2000].

Our finding that the acute deletion of *Ift20* results in opsin accumulation at the Golgi complex whereas the acute deletion of *Ift140* results in opsin accumulation in the plasma membrane of the inner segment indicates that these two proteins play different roles in the transport of opsin. Previously we found that IFT20 was unique among the IFT proteins as it is the only one that is found localized to the Golgi complex in addition to the normal localization in the peribasal body region and in the cilium itself [Follit et al., 2006; Follit et al., 2009]. We proposed that IFT20 was involved in transport or sorting of membrane proteins at the Golgi complex that are destined for the ciliary membrane compartment. Consistent with this idea, partial knockdown of *Ift20* reduced the amount of polycystin-2 in the cilium [Follit et al., 2006]. However, it was unclear if the effect on ciliary polycystin-2 level was a direct effect or was an indirect consequence of disrupting IFT. A similar criticism can be made of our prior work showing that acute deletion of *Ift20* caused opsin to accumulate at the Golgi complex. It is possible that if IFT is disrupted through the connecting cilium, opsin could back up in the Golgi complex. However, our observation that acute *Ift140* deletion causes opsin to accumulate in the plasma membrane suggests that this is not the case. These findings strongly support a model where IFT20 is involved in sorting or transport of ciliary membrane proteins from the Golgi to the base of the cilium. At the base of the cilium, IFT20 and the cargo then engage with the rest of the IFT system for transport through the connecting cilium and into the outer segment. When the rest of the IFT system is compromised by defects in subunits like IFT140, the opsin cannot be transported through the connecting cilium and remains in the inner segment.

Materials and Methods

Mouse Breeding

The *Ift140*$^{flox/flox}$ (MGI:Ift140$^{tm1c(KOMP)Wtsi}$) and *Ift140*$^{null1/+}$ (MGI: Ift140 $^{tm1b(KOMP)Wtsi}$) mice were generated and genotyped as previously described [Jonassen et al., 2012]. The generation of the HRGP-Cre line was described previously (Le *et al.*, 2004). The *rd* (*Pde6b*) mutation was bred out of the HRGP-Cre line by crosses to C57B6J (Jackson Laboratory) and genotyped as described [Pittler and Baehr, 1991]. CAG-CreER line (B6.Cg-Tg[CAG-cre/Esr1*)5Amc/J] [Hayashi and McMahon, 2002] was obtained from Jackson Laboratory. Tamoxifen (Sigma) was dissolved in peanut oil; 6 mg/~20 g mouse was delivered by oral gavage and the eyes were harvested 48 hr later. All mouse work was carried out at UMMS with approval of the Institutional Animal Care and Use Committee.

Histology

Mouse eyes were removed with a small amount of tissue above the eye for orientation and were fixed in cold PBS/4% paraformaldehyde (Electron Microscopy Sciences) for 1 hr at 4°C, followed by removal of the lens, cornea and vitreous. The eye cups were then returned to fixation in cold PBS/4% paraformaldehyde for 30 min at 4°C. Eye cups were then incubated at 4°C for 1 hr in 30% sucrose dissolved in PBS, followed by an overnight rotation in Tissue Freezing Medium (Triangle Biomedical Sciences) at 4°C. The next day,

eye cups were embedded in fresh Tissue Freezing Medium. Eighteen micron cryosections were cut from the central retina near the optic nerve, mounted on Plus slides (Fisher), blocked for 1 hr at room temp in Tris buffered saline (TBS; 10 mM Tris pH 7.5, 166 mM NaCl) supplemented with 5% goat serum and 0.1% Triton X-100, and then incubated overnight at 4°C in primary antibody diluted in blocking buffer. After washing in TBS, Alexa Fluor labeled secondary antibodies (Invitrogen) mixed with an Antibody Diluent (0.1% Fish Skin Gelatin in TBST) were used (goat anti-mouse 594 and goat anti-rabbit 488) to detect the primary antibodies. The specimens were washed in TBST (TBS with 0.1% Triton X-100), then incubated with 1 μg/μl of DAPI followed by a final wash with TBS before being mounted using Prolong Gold (Invitrogen). For cryosections, a minimum of four controls and four mutants were examined for each age group.

For paraffin embedding, mouse eyes were removed and fixed in cold PBS/4% paraformaldehyde (Electron Microscopy Sciences) for 1 hr at 4°C, followed by removal of the lens, cornea and vitreous humor. The eyes were returned to the fixative overnight at 4°C, washed with PBS, and embedded. Seven-micron sections were cut, dewaxed, rehydrated, and subjected to antigen retrieval in an autoclave with 10 mM sodium citrate at pH 9. After cooling to ambient temperature, the sections were treated with blocking solution (4% non-immune goat serum, 0.1% Triton X-100, 0.05% SDS, and 0.1% % fish skin gelatin in TBST) for 30 min, subsequently washed with TBST and then exposed to primary antibodies. IFT140 detection was enhanced by treatment with a Fab fragment of goat anti-rabbit IgG(H+L) conjugated to biotin (Jackson ImmunoResearch) followed by a Streptavidin-Alexa Fluor conjugate (Life Technologies). An Avidin/Biotin blocking kit (Life Technologies) was applied prior to the Streptavidin step. Anti-acetylated tubulin was used as cilia marker and was detected with an Alexa Fluor conjugated $F(ab')_2$ fragment of goat ant-mouse IgG(H+L). Subsequent washes were done using TBST.

For double labeling of IFT140 and cone RG-opsin with rabbit antibodies, anti-IFT140 was applied first followed by biotin-conjugated goat Fab fragment anti-rabbit IgG. A goat Fab fragment of anti-rabbit IgG (H+L) (Jackson ImmunoResearch) was then applied to saturate any remaining open sites on the IFT140 antibody. The anti-cone RG-opsin was then applied together with anti-acetylated tubulin. Fluorescent probes used were Streptavidin Alexa Fluor 568, goat $F(ab')_2$ anti-rabbit IgG(H+L) Alexa Fluor 488, and goat $F(ab')_2$ anti-mouse IgG(H+L) Alexa Fluor 647 from Life Technologies.

For immunogold EM, the lens were removed and the eye fixed overnight in 0.25% glutaraldehyde / 4% paraformaldehyde in 0.1M cacodylate buffer and then switched to 4% paraformaldehyde in 0.1M cacodylate buffer for shipment. Samples were embedded in LR White resin, and ultrathin sections were stained as described previously [Lopes et al., 2010]. Briefly, etched sections were incubated with monoclonal anti-rhodopsin antibody (1D4) overnight and goat anti-mouse conjugated to 12 nm gold (Jackson ImmunoResearch Laboratories) for 1 hr at room temperature. After secondary fixation with 2% glutaraldehyde (Electron Microscopy Sciences) sections were stained with osmium vapor, uranyl acetate and lead citrate. Images were acquired on a Zeiss TEM. Sections from experimental and control animals were processed and imaged at the same time. Immunogold particle density

along the plasma membrane and over the Golgi complex was determined using ImageJ software.

The following primary antibodies were used: cone RG-opsin (Millipore, AB5405), Cre (Sigma, clone 7-23), IFT140 [Jonassen et al., 2012], rhodopsin (Millipore, 1D4) and acetylated tubulin (Sigma, 6-11B-1). Confocal images were acquired as previously described [Jonassen et al., 2008].

Dispersed cones were generated by vortexing retinas in DMEM for 10s. Supernatant was dried onto glass slides, fixed for 15 min in 4% paraformaldehyde in PBS and then stained for IFT140 and 611-B1 followed by RG-opsin.

Accession Numbers

Ift140 (NM_134126), *Ift20* (NM_018854), RG-opsin (BC014826) and rhodopsin (NM_145383). All genes were obtained from mouse.

Data analysis

Data groups were compared using GraphPad software by one-way ANOVA (more than two groups) or unpaired t tests (two groups). Differences between groups were considered statistically significant if $p < 0.05$. Statistical significance is denoted with asterisks (*p=0.01-0.05; **p=0.001-0.01;***p<0.001). Data is plotted as mean ± standard deviation.

Acknowledgments

We thank Yun Zheng Le (University of Oklahoma Health Sciences Center) for the HRGP-Cre mice. This work was supported by the National Institutes of Health (GM060992 to GJP) and (R01EY13408 and core grant EY00331 to DSW). DSW is also supported by an RPB Jules and Doris Stein professorship. The authors have no conflicts of interest.

Abbreviations

IFT	intraflagellar transport
P	postnatal day
G	Golgi layer
IS	inner segment
OS	outer segment
NL	outer nuclear layer

References

Berbari NF, Lewis JS, Bishop GA, Askwith CC, Mykytyn K. Bardet-Biedl syndrome proteins are required for the localization of G protein-coupled receptors to primary cilia. Proc Natl Acad Sci U S A. 2008; 105:4242–4246. [PubMed: 18334641]

Besharse, JC.; Horst, CJ. The photoreceptor connecting cilium: a model for the transition zone. In: Bloodgood, RA., editor. Ciliary and Flagellar Membranes. Plenum Press; New York: 1990. p. 389-417.

Bhowmick R, Li M, Sun J, Baker SA, Insinna C, Besharse JC. Photoreceptor IFT complexes containing chaperones, guanylyl cyclase 1 and rhodopsin. Traffic. 2009; 10:648–663. [PubMed: 19302411]

Brazelton WJ, Amundsen CD, Silflow CD, Lefebvre PA. The bld1 mutation identifies the Chlamydomonas osm-6 homolog as a gene required for flagellar assembly. Curr Biol. 2001; 11:1591–1594. [PubMed: 11676919]

Cole DG, Diener DR, Himelblau AL, Beech PL, Fuster JC, Rosenbaum JL. *Chlamydomonas* kinesin-II-dependent intraflagellar transport (IFT): IFT particles contain proteins required for ciliary assembly in *Caenorhabditis elegans* sensory neurons. J Cell Biol. 1998; 141:993–1008. [PubMed: 9585417]

Fei Y. Development of the cone photoreceptor mosaic in the mouse retina revealed by fluorescent cones in transgenic mice. Mol Vis. 2003; 9:31–42. [PubMed: 12592228]

Follit JA, Tuft RA, Fogarty KE, Pazour GJ. The intraflagellar transport protein IFT20 is associated with the Golgi complex and is required for cilia assembly. Mol Biol Cell. 2006; 17:3781–3792. [PubMed: 16775004]

Follit JA, Xu F, Keady BT, Pazour GJ. Characterization of mouse IFT complex B. Cell Motil Cytoskeleton. 2009

Hayashi S, McMahon AP. Efficient recombination in diverse tissues by a tamoxifen-inducible form of Cre: a tool for temporally regulated gene activation/inactivation in the mouse. Dev Biol. 2002; 244:305–318. [PubMed: 11944939]

Insinna C, Besharse JC. Intraflagellar transport and the sensory outer segment of vertebrate photoreceptors. Dev Dyn. 2008; 237:1982–1992. [PubMed: 18489002]

Insinna C, Humby M, Sedmak T, Wolfrum U, Besharse JC. Different roles for KIF17 and kinesin II in photoreceptor development and maintenance. Dev Dyn. 2009; 238:2211–2222. [PubMed: 19384852]

Iomini C, Li L, Esparza JM, Dutcher SK. Retrograde intraflagellar transport mutants identify complex A proteins with multiple genetic interactions in Chlamydomonas reinhardtii. Genetics. 2009; 183:885–896. [PubMed: 19720863]

Jimeno D, Feiner L, Lillo C, Teofilo K, Goldstein LS, Pierce EA, Williams DS. Analysis of kinesin-2 function in photoreceptor cells using synchronous Cre-loxP knockout of Kif3a with RHO-Cre. Invest Ophthalmol Vis Sci. 2006; 47:5039–5046. [PubMed: 17065525]

Jonassen JA, San Agustin J, Follit JA, Pazour GJ. Deletion of IFT20 in the mouse kidney causes misorientation of the mitotic spindle and cystic kidney disease. J Cell Biol. 2008; 183:377–384. [PubMed: 18981227]

Jonassen JA, SanAgustin J, Baker SP, Pazour GJ. Disruption of IFT complex A causes cystic kidneys without mitotic spindle misorientation. J Am Soc Nephrol. 2012; 23:641–651. [PubMed: 22282595]

Keady BT, Le YZ, Pazour GJ. IFT20 is required for opsin trafficking and photoreceptor outer segment development. Mol Biol Cell. 2011; 22:921–930. [PubMed: 21307337]

LaVail MM. Kinetics of rod outer segment renewal in the developing mouse retina. J Cell Biol. 1973; 58:650–661. [PubMed: 4747920]

Le YZ, Ash JD, Al-Ubaidi MR, Chen Y, Ma JX, Anderson RE. Targeted expression of Cre recombinase to cone photoreceptors in transgenic mice. Mol Vis. 2004; 10:1011–1018. [PubMed: 15635292]

Lechtreck KF, Johnson EC, Sakai T, Cochran D, Ballif BA, Rush J, Pazour GJ, Ikebe M, Witman GB. The Chlamydomonas reinhardtii BBSome is an IFT cargo required for export of specific signaling proteins from flagella. J Cell Biol. 2009; 187:1117–1132. [PubMed: 20038682]

Lee JY, Ristow M, Lin X, White MF, Magnuson MA, Hennighausen L. RIP-Cre revisited, evidence for impairments of pancreatic beta-cell function. J Biol Chem. 2006; 281:2649–2653. [PubMed: 16326700]

Lopes VS, Jimeno D, Khanobdee K, Song X, Chen B, Nusinowitz S, Williams DS. Dysfunction of heterotrimeric Kinesin-2 in rod photoreceptor cells and the role of opsin mislocalization in rapid cell death. Mol Biol Cell. 2010; 21:4076–4088. [PubMed: 20926680]

Marszalek JR, Liu X, Roberts EA, Chui D, Marth JD, Williams DS, Goldstein LSB. Genetic evidence for selective transport of opsin and arrestin by kinesin-II in mammalian photoreceptors. Cell. 2000; 102:175–187. [PubMed: 10943838]

Mukhopadhyay S, Wen X, Chih B, Nelson CD, Lane WS, Scales SJ, Jackson PK. TULP3 bridges the IFT-A complex and membrane phosphoinositides to promote trafficking of G protein-coupled receptors into primary cilia. Genes Dev. 2010; 24:2180–2193. [PubMed: 20889716]

Ou G, Koga M, Blacque OE, Murayama T, Ohshima Y, Schafer JC, Li C, Yoder BK, Leroux MR, Scholey JM. Sensory ciliogenesis in *Caenorhabditis elegans*: assignment of IFT components into distinct modules based on transport and phenotypic profiles. Mol Biol Cell. 2007; 18:1554–1569. [PubMed: 17314406]

Pazour GJ, Baker SA, Deane JA, Cole DG, Dickert BL, Rosenbaum JL, Witman GB, Besharse JC. The intraflagellar transport protein, IFT88, is essential for vertebrate photoreceptor assembly and maintenance. J Cell Biol. 2002; 157:103–113. [PubMed: 11916979]

Pazour GJ, Dickert BL, Vucica Y, Seeley ES, Rosenbaum JL, Witman GB, Cole DG. *Chlamydomonas IFT*88 and its mouse homologue, polycystic kidney disease gene *Tg737*, are required for assembly of cilia and flagella. J Cell Biol. 2000; 151:709–718. [PubMed: 11062270]

Pazour GJ, Dickert BL, Witman GB. The DHC1b (DHC2) isoform of cytoplasmic dynein is required for flagellar assembly. J Cell Biol. 1999; 144:473–481. [PubMed: 9971742]

Perkins LA, Hegecock EM, Thomson JN, Culotti JG. Mutant sensory cilia in the nematode *Caenorhabditis elegans*. Developmental Biology. 1986; 117:456–487. [PubMed: 2428682]

Perrault I, Saunier S, Hanein S, Filhol E, Bizet AA, Collins F, Salih MA, Gerber S, Delphin N, Bigot K, Orssaud C, Silva E, Baudouin V, Oud MM, Shannon N, Le MM, Roche O, Pietrement C, Goumid J, Baumann C, Bole-Feysot C, Nitschke P, Zahrate M, Beales P, Arts HH, Munnich A, Kaplan J, Antignac C, Cormier-Daire V, Rozet JM. Mainzer-Saldino syndrome is a ciliopathy caused by IFT140 mutations. Am J Hum Genet. 2012; 90:864–870. [PubMed: 22503633]

Pittler SJ, Baehr W. Identification of a nonsense mutation in the rod photoreceptor cGMP phosphodiesterase beta-subunit gene of the *rd* mouse. Proc Nat Acad Sci USA. 1991; 88:8322–8326. [PubMed: 1656438]

Schmidts M, Frank V, Eisenberger T, Al TS, Bizet AA, Antony D, Rix S, Decker C, Bachmann N, Bald M, Vinke T, Toenshoff B, Di DN, Neuhann T, Hartley JL, Maher ER, Bogdanovic R, Peco-Antic A, Mache C, Hurles ME, Joksic I, Guc-Scekic M, Dobricic J, Brankovic-Magic M, Bolz HJ, Pazour GJ, Beales PL, Scambler PJ, Saunier S, Mitchison HM, Bergmann C. Combined NGS approaches identify mutations in the intraflagellar transport gene IFT140 in skeletal ciliopathies with early progressive kidney Disease. Hum Mutat. 2013; 34:714–724. [PubMed: 23418020]

Sedmak T, Wolfrum U. Intraflagellar transport molecules in ciliary and nonciliary cells of the retina. J Cell Biol. 2010; 189:171–186. [PubMed: 20368623]

Tsujikawa M, Malicki J. Intraflagellar transport genes are essential for differentiation and survival of vertebrate sensory neurons. Neuron. 2004; 42:703–716. [PubMed: 15182712]

Williams DS. Transport to the photoreceptor outer segment by myosin VIIa and kinesin II. Vision Res. 2002; 42:455–462. [PubMed: 11853761]

Williams DS. Usher syndrome: animal models, retinal function of Usher proteins, and prospects for gene therapy. Vision Res. 2008; 48:433–441. [PubMed: 17936325]

Young RW. The renewal of photoreceptor cell outer segments. J Cell Biol. 1967; 33:61–72. [PubMed: 6033942]

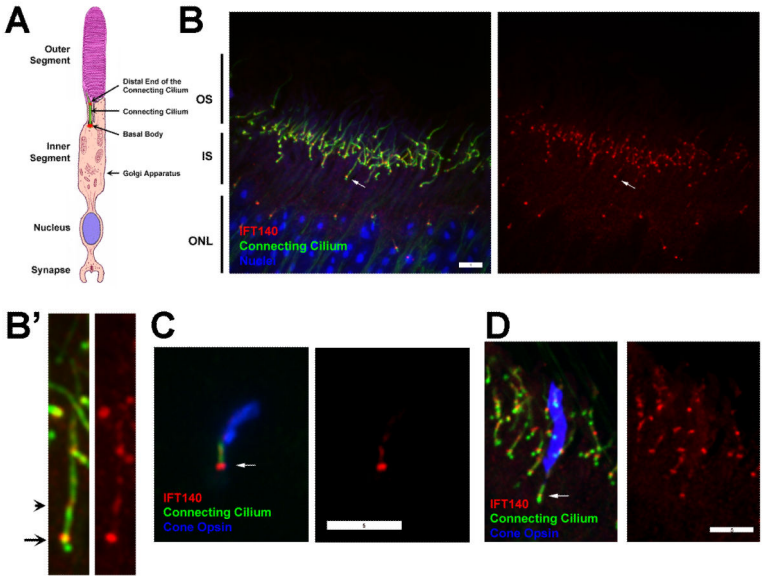

Figure 1. IFT140 in photoreceptors

A. Diagram of a photoreceptor rod cell. Image is modified from [Williams, 2008].

B. Paraffin section from a wild type P28 animal stained for IFT140 (red), cilia (6-11B-1, anti-acetylated tubulin, green) and DAPI (blue). The retina is oriented similar to the drawing in **A**. Arrow points at the basal body end of a connecting cilium. Images are maximum projections of 17 image Z-stacks taken at 0.25 μm intervals. Scale bar is 5 μm. **B'.** 4X enlargements of the cell marked with an arrow in **B**. Arrow points at the basal body end of the cilium, arrow head points at the presumed distal end of the connecting cilium.

C. Dispersed cone cell from a wild type P28 animal stained for IFT140 (red), cilia (6-11B-1, green) and RG-opsin (blue). Scale bar is 5 μm. Arrow marks the basal body.

D. Paraffin section of a wild type animal stained for IFT140 (red), cilia (6-11B-1, green) and RG-opsin (blue). Scale bar is 5 μm. Arrow marks the basal body region of the cone cell.

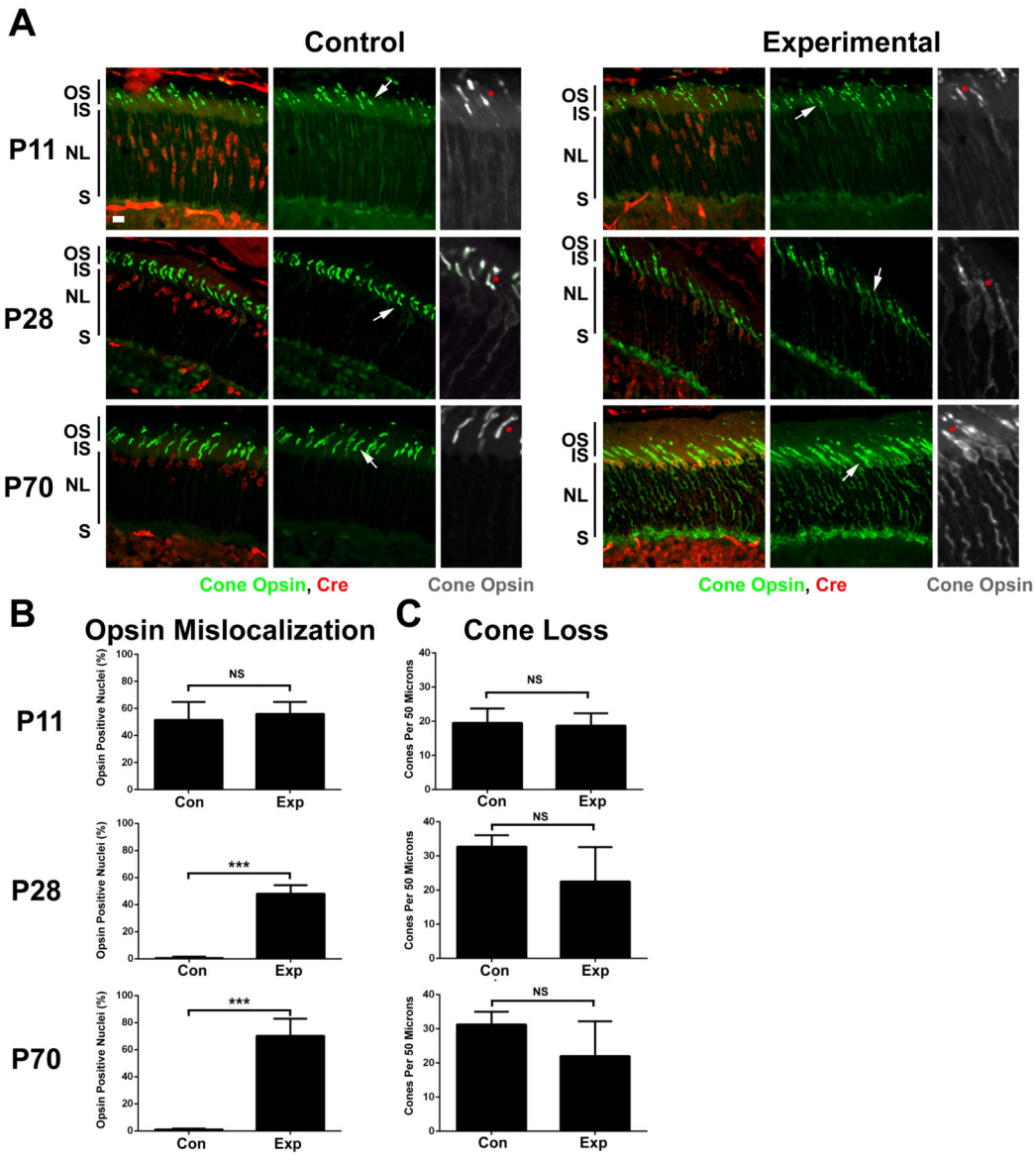

Figure 2. Deletion of *Ift140* leads to cone cell degeneration

A. Cryosections from P11 (top row), P28 (middle row) and P70 (bottom row) control (*Ift140*$^{flox/null1}$, *HRGP-Cre+*, left panels) and experimental (*Ift140*$^{flox/+}$, *HRGP-Cre+*, right panels) animals. Sections were stained with RG-opsin (green) and Cre (red). Scale bar is 10 μm and applies to all images in A. Grey scale images are 2X enlargements of the RG-opsin channel from the region at the arrow. * mark outer segments. Note that the red label in the inner nuclear layer (below the outer plexiform layer) is present in Cre-negative animals and does not indicate that Cre is expressed in these cells. Images are maximum projections of 10 image Z-stacks taken at 0.5 μm intervals. IS, inner segment; OS, outer segment; NL, outer nuclear layer; S, ribbon synapse.

B. Percentage of Cre+ nuclei that were surrounded by RG-opsin was determined from cryosections obtained from at least four control and four experimental animals at each time point. NS, not significant; *** $p<0.001$.

C. Number of cone outer segments in a 50 μm interval was counted from at least four control and four experimental animals at each time point. NS, not significant.

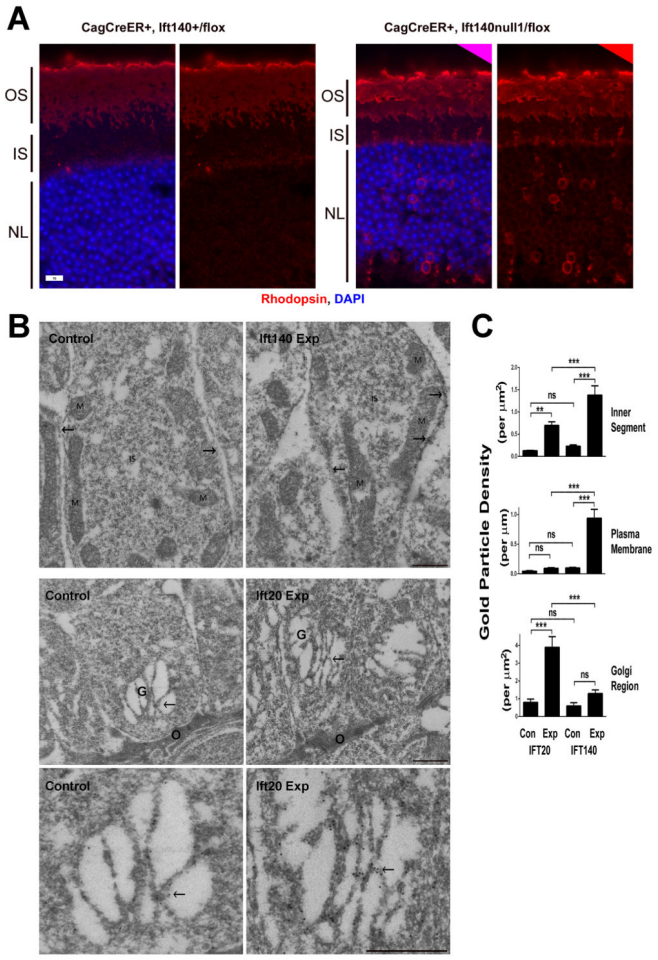

Figure 3. Acute deletion of *Ift140* causes opsin accumulation in the plasma membrane

A. Paraffin section of control and experimental retinas harvested 48 hr after administration of tamoxifen. Note the accumulation of rhodopsin (red) in the inner segment (IS) and around the nuclei (blue, NL) in the experimental animals. OS, outer segment. Scale bar is 10 µm.

B. Immunogold labeling of rhodopsin of *Ift140* (top row) and *Ift20* (middle and bottom row) control and experimental retinas harvested 48 hr after administration of tamoxifen. Arrows indicate plasma membrane in the upper row and the Golgi complex (G) in the middle and bottom row. The upper row shows sections through the distal region of the inner segment (IS); M, mitochondria. The middle row shows sections through the proximal region of the inner segment; the outer limiting membrane (O) represents the proximal limit of the inner segment and consists of adherens junctions between adjacent photoreceptor cells and Mueller cells. The lower row are higher magnification micrographs of the Golgi complexes shown in the middle row. Scale bars are 500 nm.

C. Quantification of gold particles. Units are per micron squared for the inner segment and Golgi region and per micron for the plasma membrane. ns, not significant; *p=0.01-0.05; **p=0.001-0.01;***p<0.001.